Journal of Applied Polymer Science

Preparation and Dielectric Behavior of Polyvinylidene Fluoride Composite Filled with Modified Graphite Nanoplatelet

Pincheng Xie,[1] Yuchao Li,[2] Jun Qiu[1]
[1]School of Materials Science and Engineering, Tongji University, Shanghai 201804, People's Republic of China
[2]School of Materials Science and Engineering, Liaocheng University, Shandong 252059, People's Republic of China
Correspondence to: J. Qiu (E-mail: qiujun@tongji.edu.cn)

ABSTRACT: Graphite nanoplatelet (GNP) was modified by polyvinylpyrrolidone (PVP), Cetyltrimethyl ammonium bromide (CTAB), γ-aminopropyltriethoxysilane (KH-550), and Stearic acid (SA), respectively. The polyvinylidene fluoride (PVDF)/modified GNP (m-GNP) nanocomposites were fabricated via solution mixing method. SEM, TEM, XRD, FTIR, and impendence analyzer were used to characterize the morphology, structure, and their electrical properties. Results showed that PVP and CTAB modified-GNP enables a better homogeneous dispersion of GNP in *N,N*-dimethylformamide (DMF) solvent than that of KH-550 and SA, which leads to a decreased conductivity in PVDF/m-GNP system. The permittivities of these nanocomposites were found to decrease with increasing frequencies. The SA modified-GNP filled PVDF nanocomposite has the largest dielectric constant and lowest dielectric loss. Such electrical behavior can be well interpreted in terms of the percolation theory. © 2013 Wiley Periodicals, Inc. J. Appl. Polym. Sci. **2014**, *131*, 40229.

KEYWORDS: nanotubes; graphene and fullerenes; nonpolymeric materials and composites; dielectric properties

Received 23 October 2013; accepted 23 November 2013
DOI: 10.1002/app.40229

INTRODUCTION

With rapid development in electronic industry, much work has been paid on the fabrication of electronic devices with enhanced dielectric constant (high-K), superior mechanical strength, and processability. Polymer-based nanocomposites have advantages over traditional perovskite ceramics for its excellent processability and low dielectric loss.[1,2] One of the most important parameters to evaluate a capacity is the ability to storage electric energy (W), which is proportional to capacitance (C), and voltage (U) according to the following formula: $W = 1/2CU^2$. For the electrical double layer capacitors (EDLC), its capacitance (C) is proportional to the surface area (S) of the layer and to the permittivity (ε) of the dielectric material and inversely proportional to the thickness (d) of the double layer as expressed by $C = S\varepsilon/d$.[3,4] Therefore, the storage of electric energy for a given sample is directly determined by the dielectric constant (ε). As recognized, neat polymers are hardly to be used as capacitors due to the limitation of its low dielectric constant. Such high permittivity polymeric materials can be realized by adding piezoelectric high-K ceramic particles, such as barium titanate ($BaTiO_3$), lead titanate ($PbTiO_3$), and lead zirconium titanate (PZT).[5] Dang et al. has reported a solution fabricated PVDF/$BaTiO_3$ composites with a dielectric constant of 40.74 at 50 vol % $BaTiO_3$ concentrations.[6] However, high filler loadings generally impair mechanical properties of polymer composites, thus limiting their practical applications.

Recently, high-K performance and light weight polymer composites can be successfully achieved by incorporating conductive fillers such as carbon nanotube, metals, graphene, et al.[1,7–11] Consequently new numerical methods were presented to predict the apparent dielectric constant and effective transport properties of multiphase functionally graded materials by Wang et al.[12–14] The permittivity of such materials is found to increase dramatically near the percolation threshold.[15] However, such composites are accompanied with a large dielectric loss due to the formation of conductive filler network. In this regard, our strategy in this work is to use some insulated molecules to modify the conductive fillers (GNP). For one thing, the well dispersed GNP in polymer matrix may be more effective in forming large quantities of minicapacitors in polymer matrix, thus leading to a large dielectric constant. For another, the large molecules attached on GNP surface prevents the formation of conductive network, which may effectively decrease the dielectric loss of a composite.

PVDF is a kind of semicrystal thermoplastic polymer with serial crystalline phases, such as α, β, γ, and δ. The β-phase is very attractive for many applications due to its good piezoelectric and pyroelectric properties. Graphite nanoplatelet (GNP, with

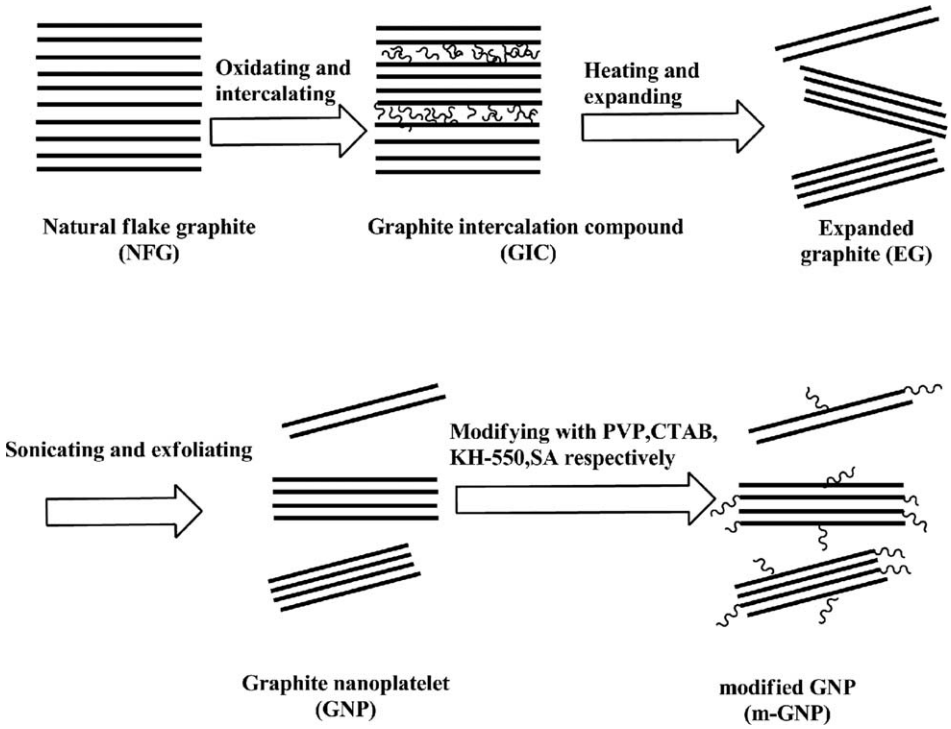

Scheme 1. Schematic illustration of preparing m-GNP from NFG.

thicknesses of roughly 10 nm and lateral dimensions as large as 15 μm) typically derived from graphite intercalation compounds (GICs) has exhibited exceptional thermal, mechanical, and electrical properties.[16] There are also several reports giving experimental evidence of a rise in the dielectric constant of PVDF in the neighborhood of the percolation threshold.[1,9,17,18]

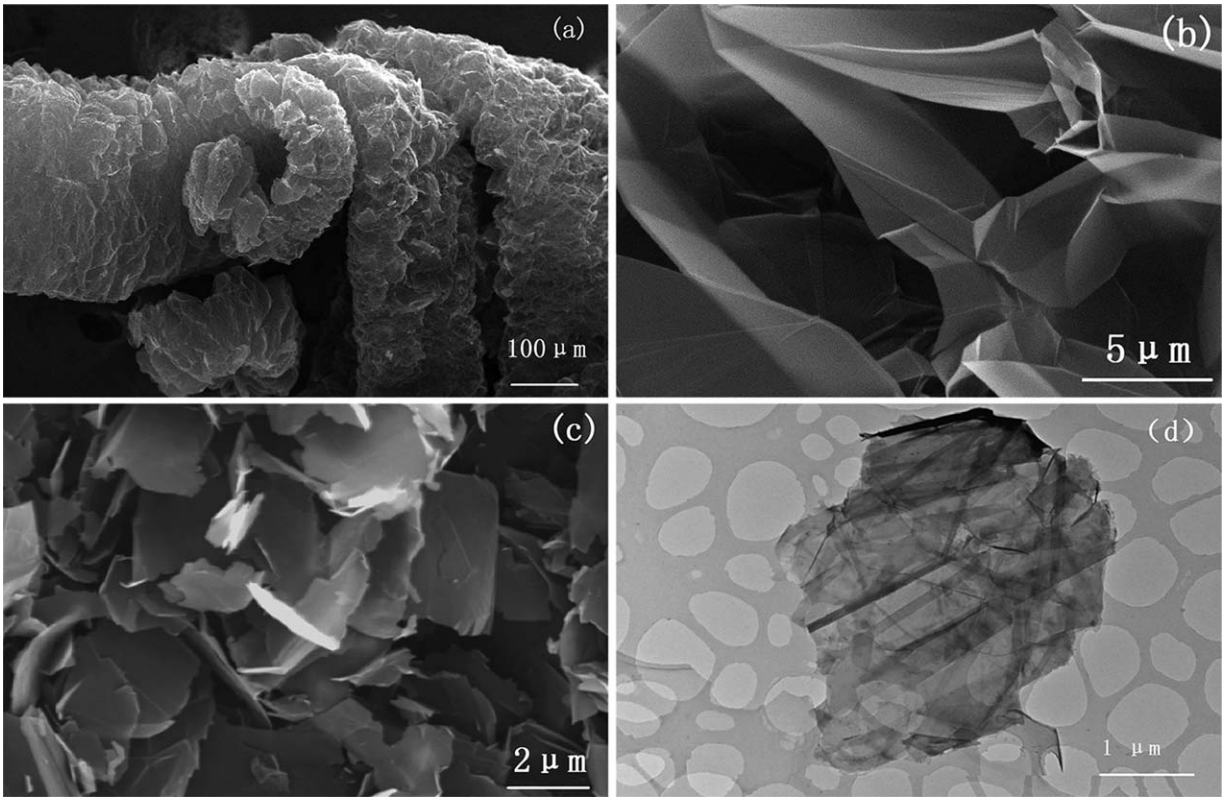

Figure 1. SEM images of (a) low and (b) high magnification of EG; (c) GNP; (d) TEM images of GNP.

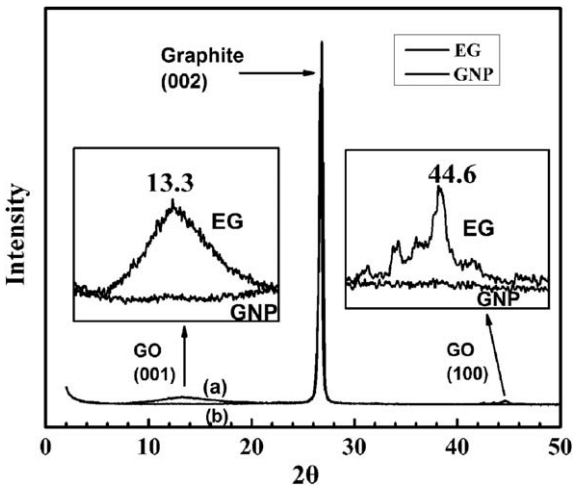

Figure 2. XRD Patterns of (a) EG and (b) GNP; the insets show local amplification at $2\theta = 13.25°$ and 44.65°, respectively.

In our previous work, a large dielectric constant of 173 was observed in the PVDF/2.5 wt % GNP nanocomposite.[18] In this work, 2.5 wt % GNP content is selected for fabricating PVDF/GNP nanocomposites. The objective of this article is to evaluate the effectiveness of various modifications of GNP on the electrical performance of PVDF/GNP nanocomposite, from which we expect it could provide further guidance for providing a solution or improvement for all the above mentioned limitations and issues.

EXPERIMENTAL

Preparation of Modified Graphite Nanoplatelet (m-GNP)

The natural flake graphite (NFG) with an average diameter of 500 μm (from Shandong Qingdao Company of China) was dried at 50°C in a vacuum oven for 48 h. The dried NFG was subsequently ultrasonicated in fuming nitric acid, potassium permanganate and citric acid solutions for 30 min. The resulting graphite intercalation compound (GIC, the so-called expandable graphite) was then washed to pH7 by deionized water and dried at 50°C in a vacuum oven 3 days. The dried GIC was rapidly expanded with intensive heating in a microwave oven, producing a loose material commonly referred to the expanded graphite (EG). The resulting EG was followed by exfoliation into GNP in an alcohol based solvent (CH_3CH_2OH : H_2O = 70 : 30, vol %) under sonication for 12 h.

The prepared GNP was immersed in polyvinylpyrrolidone (PVP), cetyltrimethyl ammonium bromide (CTAB), 3-aminopropyltri ethoxysilane (KH-550), and Stearic acid (SA) solvent with conti nuous stirring and ultrasonication for 2 days, respectively. The fi nal product was filtered and the modified PVP-GNP, CTAB-GNP, KH-GNP, and SA-GNP were fabricated. The schematic illustration of synthesizing m-GNP is shown in Scheme 1.

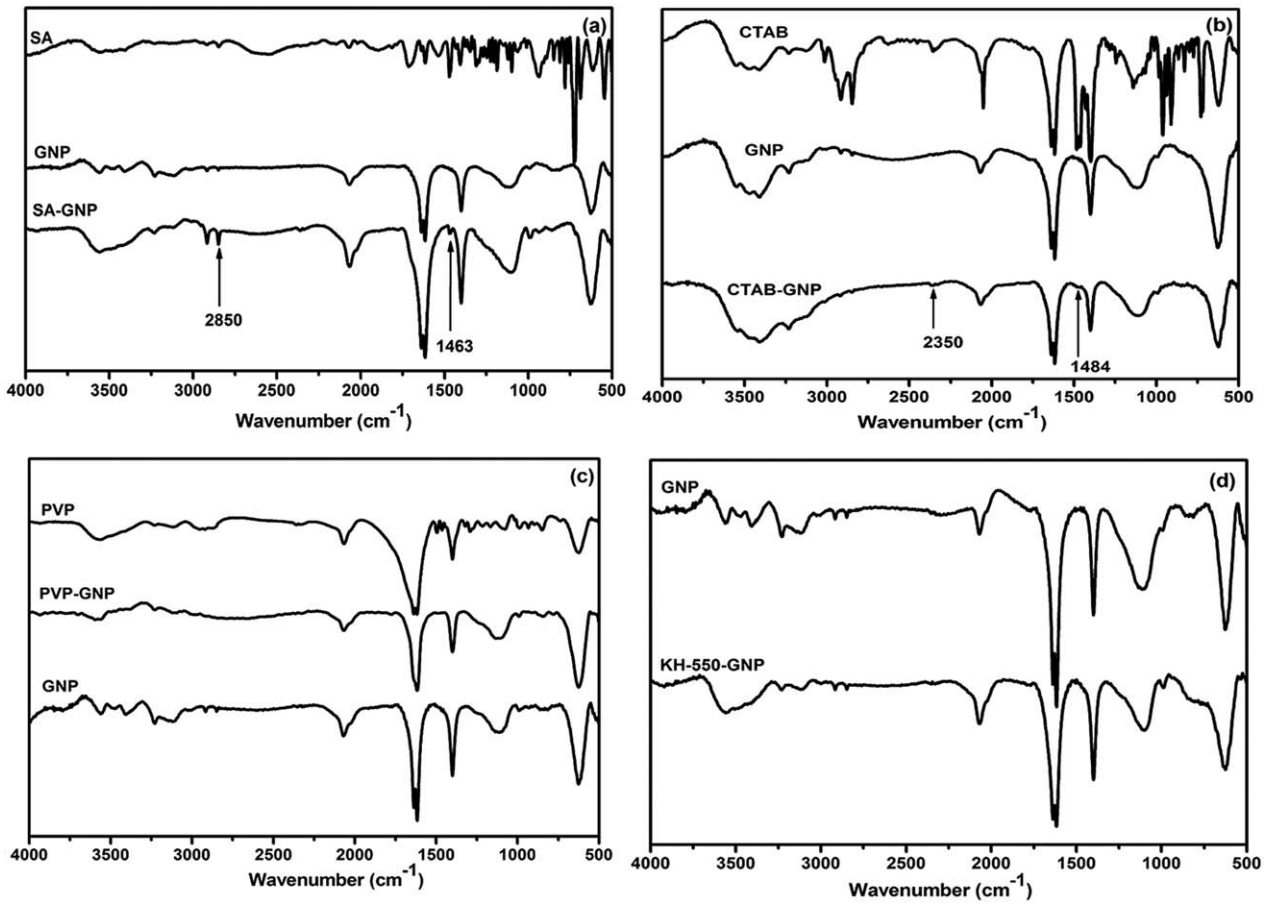

Figure 3. FTIR Spectra of (a) SA-modified GNP; (b) CTAB-modified GNP; (c) PVP-modified GNP; (d) KH-550-modified GNP.

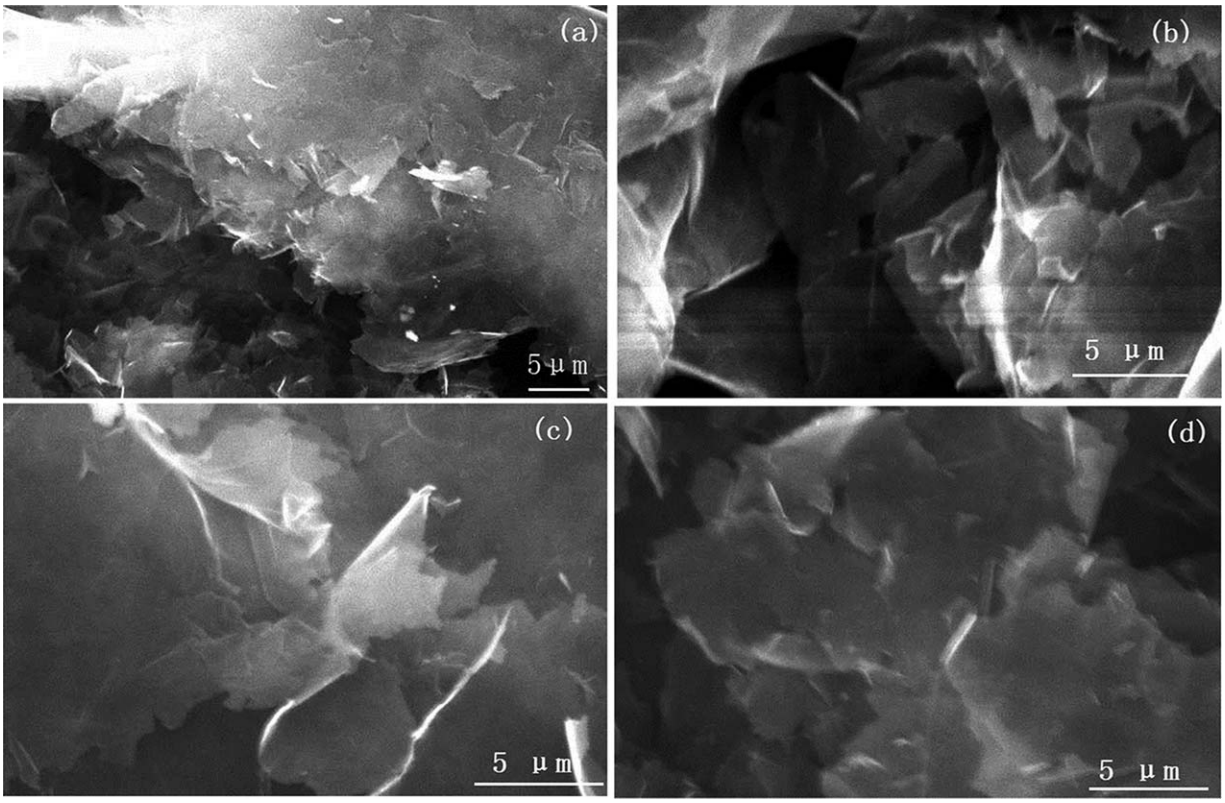

Figure 4. SEM images of (a) SA-modified GNP; (b) CTAB-modified GNP; (c) PVP-modified GNP; (d) KH-550-modified GNP.

Fabrication of m-GNP/PVDF Nanocomposites

The m-GNP/PVDF nanocomposites were fabricated via solution mixing methods. Briefly, PVDF was firstly dissolved in *N,N*-dimethylformamide (DMF) solvent. A stoichiometric amount of m-GNP was added to the mixture. The weight ratio of PVDF/GNP was kept at 97.5/2.5. The mixture was sonicated for 4 h in order to form a homogeneous dispersion. The PVDF/m-GNP nanocomposites were obtained after evaporation of DMF solvent at 60°C overnight. Finally the resulting nanocomposites were compression-molded at 220°C under the pressure of 10 MPa.

Characterization and Measurement

Pristine X-ray diffraction (XRD) measurements were performed at room temperature in a Philip X'pert diffractometer (Philips X'pert PW-3020) using Cu Kα radiation with the 2θ ranging from 2° to 50°. Scanning electron microscopy (SEM, JEOL JSM-820, JEOL, Tokyo, Japan) and transmission electron microscopy (TEM, Tecnai F30, FEI, The Netherlands) were used to observe the microstructure of EG and GNP. The morphology of m-GNP/PVDF nanocomposite was also revealed by SEM. The structure of m-GNP was studied using FTIR (Nicolet IR-100, USA) with pressing potassium bromide troche.

Disk-shaped samples of 6 mm in diameter were coated with silver paste on both sides of the molded specimens (0.5 mm in thickness). The electrical properties of the sample were measured with an HP 4294A precision impedance analyzer (Agilent Inc., USA) with frequency ranging from 50 Hz to 50 MHz at room temperature.

RESULTS AND DISCUSSION

The Structure of GNP

The SEM micrographs of EG was shown in Figure 1(a,b), from which the loosely stacked structures of EG was observed. It can also be revealed from Figure 1(b) that there are many pores with micron scales in diameter in a larger magnification. The thin platelets of EG are connected with each other and not exfoliated to single sheets. It is mainly attributed to the heterogeneous expansion of GIC.

The two-dimensional geometry of GNP was shown in Figure 1(c). It can be seen that the tangled platelets were exfoliated absolutely under the treatment of ultrasonication in alcohol solvent. The average lateral dimension of GNP was as large as about 10 μm. Figure 1(d) shows the TEM image of GNP. It is seen that the thickness of GNP was exfoliated roughly into nanoscale dimensions.

Figure 2 shows the XRD patterns of EG and GNP. Both EG and GNP showed the characteristic peak ($2\theta = 26°$) of the (002) crystal face of graphite, indicating that EG and GNP have the graphite layer structure as NFG. The peaks located at $2\theta = 13.25°$ and 44.65° are characteristic reflections of GIC. They are assigned to the (001) and (100) crystal face of Graphite Oxide (GO), respectively. However, the two peaks disappeared

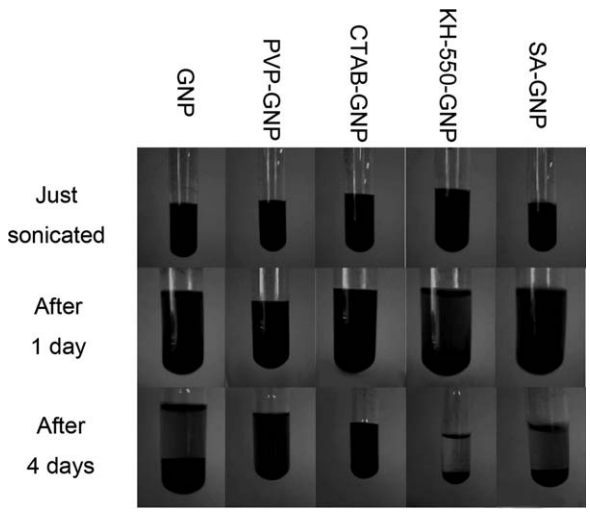

Figure 5. Digital pictures of as-prepared m-GNP dispersed in DMF solvent through bath ultrasonication. Top: dispersions immediately after sonication. Mid: dispersions 1 day after sonication. Bottom: dispersions 4 days after sonication.

in the XRD patterns of GNP indicating thorough expansion of GIC after thermal treatment.

Characterization of m-GNP

Figure 3 shows the FTIR Spectra of various m-GNPs. The FTIR spectra of SA-GNP [Figure 3(a)] and CTAB-GNP [Figure 3(b)] retained most of the bands of SA and CTAB, respectively. In the spectrum of SA-GNP, the bands centered at 2912 cm^{-1} and 1463 cm^{-1} are strengthened, indicating significant contribution from the antisymmetric vibration (2912 cm^{-1}) and in-plane and out-plane bending(1463 cm^{-1}) of the C—H unit in SA. The development of the band at 1484 cm^{-1} [Figure 3(b)] is attributed to C—N stretching of CTAB. In addition, there is also weak increase in the band around 2350 cm^{-1}, which also appears markedly in neat CTAB. However, it is difficult to observe any characteristic peaks from the spectra of PVP-GNP [Figure 3(c)] and KH-550-GNP [Figure 3(d)], indicating ineffective modification of GNP. The morphology of m-GNP was presented in Figure 4(a–d). It can be observed distinctly that most of the tangled platelets have been exfoliated.

To further investigate the dispersion state of m-GNP, the as-prepared m-GNP was dispersed in DMF with the aid of ultrasonication treatment for 1 h. Figure 5 shows digital pictures of the dispersions immediately (top), 1 day (mid), and 4 days (bottom). It can be noticed that various m-GNPs can well dispersed in DMF solvent after sonication. However, many of these dispersions displayed only short-term stability and precipitated gradually in one day or two, especially for KH-550 and SA modified GNP. A better dispersion was obtained in the CTAB modified GNP solvent. The solution exhibited a long-term stability even after 4 days deposition. As shown in Figure 6(a−d), GNPs are found to disperse homogeneously in the matrix of PVDF after modification, thus leading to the excellent electrical performance as follows.

Electrical Performance of m-GNPs/PVDF Nanocomposites

Figure 7 shows the electrical properties of m-GNP/PVDF nanocomposites. From Figure 7(a), the electrical conductivities of

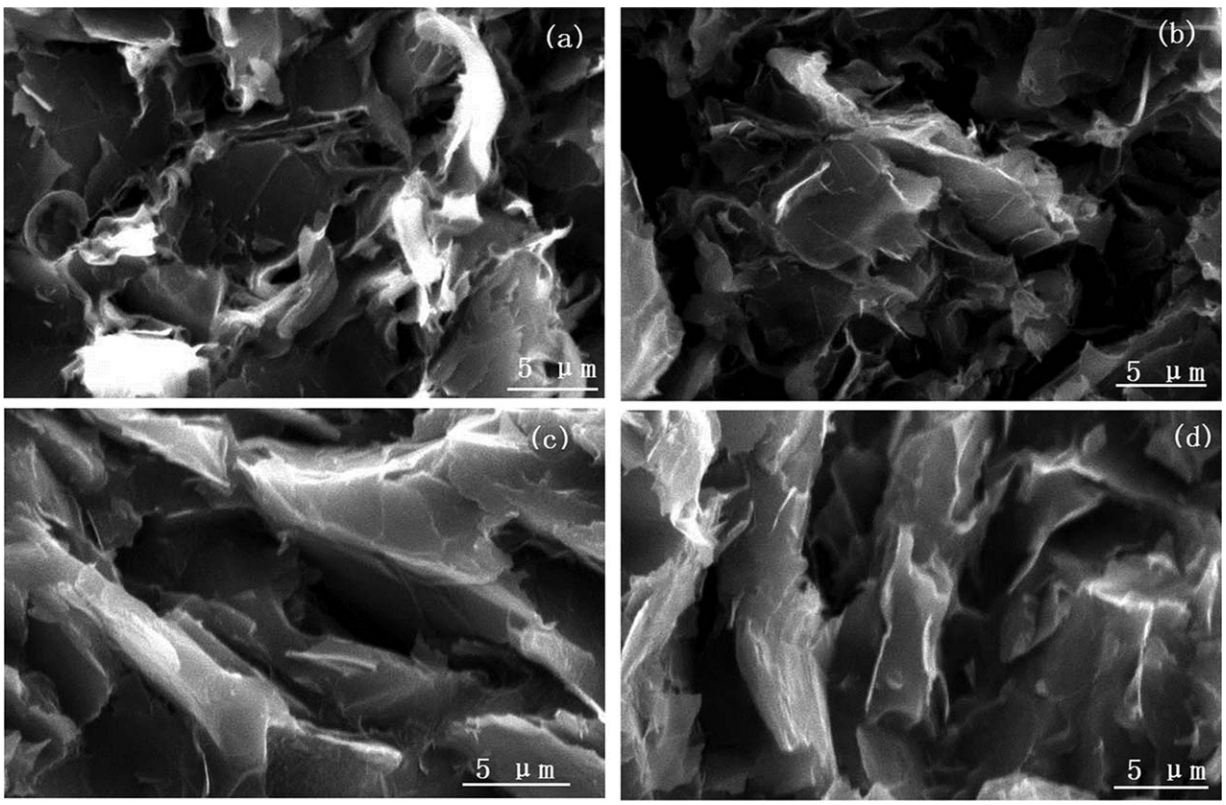

Figure 6. SEM images for (a) SA-GNP/PVDF; (b) CTAB-GNP/PVDF; (c) PVP-GNP/PVDF; (d) KH-550-GNP/PVDF composites.

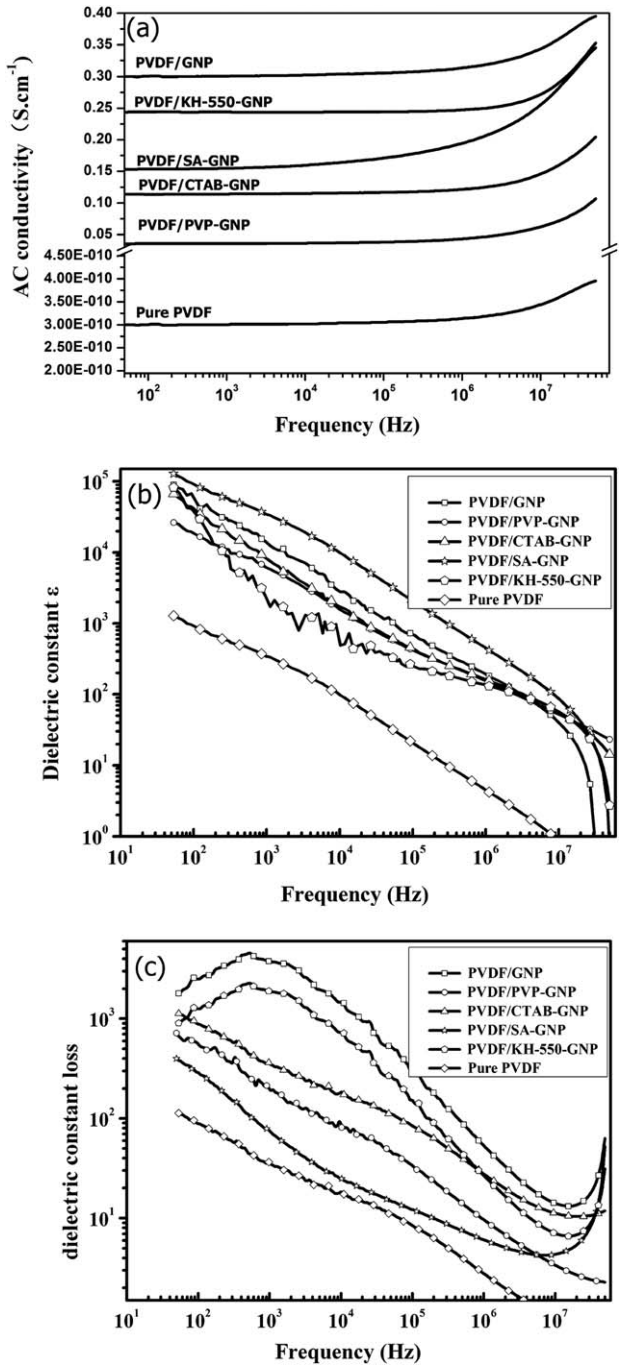

Figure 7. Electrical conductivity σ; (b) dielectric constant ε and (c) dielectric constant loss tanδ of the m-GNP /PVDF composites as a function of frequency f.

these m-GNP/PVDF composites have been significantly improved by several orders of magnitude as compared with that of neat PVDF. It can be explained that 2.5 wt % GNP additions in the nanocomposite can reach the percolation threshold, where a conductive network of filler particles is formed. However, the conductivity of m-GNP/PVDF nanocomposites is slightly reduced as compared with that of GNP/PVDF system which indicates that the modification of GNP will hinder the formation of conductive network. The better modification of GNP leads to a larger decrease in conductivity as evidenced from the curves of PVDF/CTAB-GNP and PVDF/PVP-GNP.

Figure 7(b) shows the variation of dielectric constant (ε') as a function of frequency. The dielectric constant shows a sharp drop with increasing of applied frequency for all nanocomposites. It is attributed to the fact that the dipole relaxation of the nanocomposites lags behind the rapid change of external frequencies. According to the percolation theory, the conductivity and permittivity obey the power law relationship with external frequencies : $\sigma \propto \omega^u$, $\varepsilon \propto \omega^{u-1}$, where $\omega = 2\pi f$ and u is the critical exponent and theoretically $u = 0 \sim 1$.[6,19] In this regard, only SA-GNP/PVDF exhibits enhanced dielectric constant compared with that of GNP/PVDF. It is because of the fact that SA-GNP filler in the PVDF matrix is in very close proximity to one another, but remains approximately insulated owing to the insulated SA molecules on its surface. And such micro morphology of SA-GNP can be more effective in forming large quantities of minicapacitors in its corresponding nanocomposite.

The plots of loss tangent (tanδ) as a function of frequency are shown in Figure 7(c). GNP/PVDF exhibits quite high loss tangent. However, a distinct drop in dielectric loss for the m-GNP/PVDF nanocomposites can be observed at high frequencies. Interestingly, SA-GNP/PVDF showed the lowest dielectric loss, thus making this kind of nanocomposite particularly attractive for practical applications. According to the literature,[9] the loss tangent can be expressed as: $\sigma = \varepsilon^o \omega \varepsilon'$ tanδ, where ε^o is the permittivity of free space and ε' is the real permittivity. By comparing the electrical conductivity σ [Figure 7(a)] and dielectric loss tanδ [Figure 7(c)], it can be found that the results are in good agreement with the equation above. From the analysis above, it can be further confirmed that the modification of GNP weakened the electrical conductivity and also have a great beneficial effect on dielectric loss of the composite by lowering it as compared to GNP/PVDF composite.

CONCLUSIONS

A two-phase percolative composites with conductive phase (modified graphite nanoplatelets, m-GNP) embedded into the PVDF matrix has been fabricated via solution mixing method followed by compression hot-molding process. Digital pictures of m-GNP in DMF solvents indicated the effective modification of GNP by PVP and CTAB. Electrical measurements showed that the electrical conductivity increased slightly while the dielectric constant decreased sharply with increasing frequency, which is conformed to the percolation theory. What's more, SA modified-GNP-filled PVDF nanocomposite exhibited the largest dielectric constant and lowest dielectric loss.

ACKNOWLEDGMENTS

This work was financially supported by Doctoral Research Foundation (No. BS2011CL012) form the Science and Technology Commission of Shandong Province, PRC.

REFERENCES

1. Li, Y. C.; Tjong, S. C.; Li, R. K. Y. *Express Polym. Lett.* **2011**, *5*, 526.

2. Rao, Y.; Ogitani, S.; Kohl, P.; Wong, C. P. *J. Appl. Polym. Sci.* **2002**, *83*, 1084.
3. Frackowiak, E.; Beguin, F. *Carbon* **2001**, *39*, 937.
4. Bai, Y.; Cheng, Z. Y.; Bharti, V.; Xu, H. S.; Zhang Q. M. *Appl. Phys. Lett.* **2000**, *76*, 3804.
5. Li, Y. C.; Ge, X. C.; Wang, L. P.; Wang, L. F.; Liu, W.; Li, H.; Li, R. K. Y.; Tjong, S. C. *Curr. Nanosci.* **2013**, *679*, 9.
6. Dang, Z. M.; Shen, Y.; Nan, C. W. *Appl. Phys. Lett.* **2002**, *81*, 4814.
7. Bhattacharya, S. K.; Chaklader, A. C. D. *Polym. Plast. Technol.* **1982**, *19*, 21.
8. Bhattacharya, S. K.; Chaklader, A. C. D. *Polym. Plast. Technol.* **1983**, *20*, 35.
9. Li, Y. C.; Tjong, S. C. *Curr. Nanosci.* **2012**, *8*, 732.
10. Li, Y. C.; Li, R. K. Y.; Tjong, S. C. *J. Nanomater.* **2009**, 2010, 39.
11. Tjong, S. C. *Key Eng. Mater.* **2012**, *495*, 5.
12. Wang, M. R.; Pan, N. *J. Appl. Phys.* **2007**, *101*, 114102.
13. Wang, M. R.; Meng, F. K.; Pan, N. *J. Appl. Phys.* **2007**, *102*, 033514.
14. Wang, M. R.; Pan, N. *Mater. Sci. Eng. R.* **2008**, *63*, 1.
15. Baudot, C.; Tan, C. M. *Carbon* **2011**, *49*, 2362.
16. Potts, J. R.; Dreyer, D. R.; Bielawski, C. W.; Ruoff, R. S. *Polymer* **2011**, *52*, 5.
17. Zheng, W. G.; Wong, S. C. *Compos. Sci. Technol.* **2003**, *63*, 225.
18. Li, Y. C.; Tjong, S. C.; Li, R. K. Y. *Synth. Met.* **2010**, *160*, 1912.
19. Nan, C. W. *Prog. Mater. Sci.* **1993**, *37*, 1.